The Mechanism of Naphthalene Decomposition in Corona Radical Shower System by DC Discharge

GAO Xiang[1], SHEN Xu[1], WU Zuliang[1,2], LUO Zhongyang[1], NI Mingjiang[1] CEN Kefa[1]
(1 State Key Laboratory of Clean Energy Utilization of Zhejiang University, Hangzhou, 310027, PR China
E-mail: xgao@zju.edu.cn
2 College of Environmental Science and Engineering of Zhejiang Gongshang University, Hangzhou, 310012, PR China
E-mail: wuzuliang@zju.edu.cn)

Abstract: Polycyclic aromatic hydrocarbons (PAHs) from coal-fired boilers and waste incinerators are regarded as some toxic and difficult decomposition pollutants. In this paper, it was studied how the applied voltage, the initial concentration and the catalyst affected the naphthalene decomposition characteristics using a corona discharge radical shower system. The emission spectrum of OH ($A^2\Sigma^+ \rightarrow X^2\Pi$) was detected to understand the decomposition mechanism of naphthalene better. In addition, the decomposition by-products and the decomposition process were also analyzed initially. The results show that the increasing applied voltage and humidity is helpful to the naphthalene decomposition because of the increasing OH radicals. High initial concentration of naphthalene can heighten the decomposition amounts and the catalyst can improve the naphthalene decomposition. The main decomposed by-product is CO_2 and H_2O. However, there are also little CO and small-molecule organic compounds to be found because of the incompletely oxidative reactions.

Keywords: naphthalene, decomposition, corona radical shower, OH, emission spectrum

1 INTRODUCTION

Currently, the removal of polycyclic aromatic hydrocarbons (PAHs) from coal-fired boilers and waste incinerators is paid more and more attention with stricter environmental standard [1-3], because PAHs endanger human health and environmental safety badly. Thought there are many technologies such as absorption, biology restoring and oxidation used for PAHs removal, the effect is not perfect. The reason is that the decomposition process of PAHs has not been clearly investigated.

The plasma flue gas treatment technology has been applied in the last decade [4-7]. In this paper, naphthalene was chosen as a typical PAH. The corona radical shower (CRS) technology is one of the most efficient plasma pollutant removal technologies. In the CRS system, a pipe electrode with nozzles was used as a discharge electrode. Additional gases (such as O_2, H_2O, etc) were injected into the reactor through the nozzle. Because of intensive electric field around the tip of nozzle, the additional gases from nozzles were dissociated into various active species (such as OH, O, O_3, etc). These radicals can converse pollutant into harmful compounds [8,9].

In order to investigate the process of naphthalene decomposition, OH radical as an important active species was detected by an optical emission spectroscopy system. The optical emission spectroscopy (OES) diagnosis is a simple and dependable method for radical measurement. Many studies on OH radical diagnosis have been reported [10,11]. In this work, the OES method was used to diagnose OH radical in the corona radical shower system. Additionally, the decomposition by-products were detected in order to understand the decomposition process better.

2 EXPERIMENT SYSTEM AND SETUP

The schematic diagram of experimental apparatus is showed in Fig. 1. The simulated flue gas system consists of an additional gas system, a CRS reactor, a treated gas analyzed system and an emission optical detection system. The inside size of CRS reactor is 200 mm×50 mm×50 mm made of plexiglass. Two plate electrodes of stainless steel were adhered to the reactor inner as negative poles. A stainless steel pipe with four pairs of nozzles (5 mm length, 2 mm outer diameter, 1.8 mm inner diameter) was used as positive electrode. A quartz window was mounted on one side for optical measurement. The nozzle-to-plate spacing was 20 mm. The positive high voltage was applied to the nozzle to form positive corona.

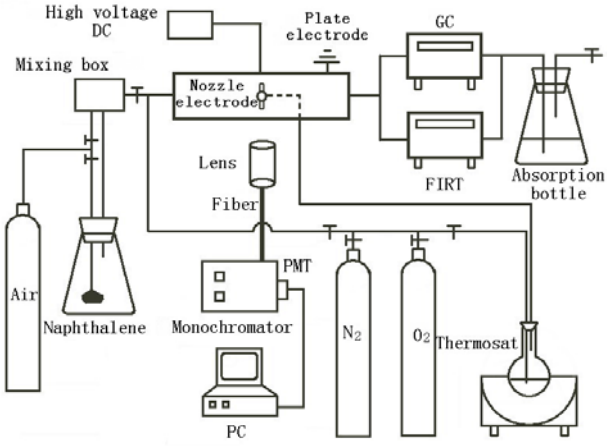

Fig. 1 Experimental system

In the simulated flue gas system, air containing naphthalene was introduced into the reactor. The explosive limit of naphthalene is 0.88%-5.9% (v/v). Therefore, in order to control the concentration of naphthalene strictly, naphthalene was wrapped in the gauze so as to limit its volatilization. In the experiment, the flux of flue gas was 5L/min (RH=70%). The additional gas was humid O_2 and the flux was 0.5 L/min. The treated gas was analyzed by gas chromatography (GC9790, FID, DB-624 capillary column Wenlin Fuli Co., China) and Fourier Transform Infrared Spectroscopy (Necolet nexus spectrometer).

For the detection of OH radical, both the simulated flue gas and the additional gas was N_2. The emission optical detection system included a quartz lens group (ϕ =25.4, f=38.1 mm; ϕ =25.4, f=75 mm), a high precision electric platform (0.625 μm minimum step) and a Zolix SBP 300 Spectrometer (1200 L/mm grating groove, 350nm glancing wavelength; a CR131 PMT tube).

3 RESULTS AND DISCUSSION

3.1 The Effect of Applied Voltage

Tab.1 shows the effect of applied voltage and initial concentration on naphthalene reduction. It is obtained that the decomposing rate of naphthalene decreases from 69% to 35% when the initial concentration increases from 17 mg/m^3 to 50 mg/m^3. However the decomposing amounts increase from 3.87 mg/h to 5.87 mg/h. Therefore the decomposing rate decreases and the decomposing amounts increase with the initial concentration of naphthalene under the same applied voltage. The results can be explained as follow: when the generating rate of active radical is not changed under the same applied voltage, the collision ratio between radical and naphthalene increases with the increasing initial concentration of naphthalene. Therefore, the positive reactions between radical and naphthalene accelerate and the decomposing amounts increase.

Table 1 Naphthalene decomposition effect

No.	Initial concentration (mg/m^3)	Applied voltage (kV)	Decomposing amounts (mg/h)	Decomposing rate (%)
1	17	8	1.8	32
2	17	11	2.81	50
3	17	14	3.87	69
4	31	14	5.42	53
5	50	14	5.78	35

From Table 1, it is also indicated that the decomposing rate of naphthalene improves as the applied voltage increases. The reason is that the increasing applied voltage improves corona discharge and the discharge current also increases. Thus, the increasing generation rate of radical improves the decomposition of naphthalene.

In the process of naphthalene decomposition, OH radical is very important. In this section, the influence of applied voltage on the generation of OH radical was investigated and the emission spectrum method was used. In the experiment of OH detection, the simulated flue gas is N_2 (Q_1=5 L/min) and the additional gas is humid N_2 (Q_2=0.5 L/min, RH=80%). Fig. 2 illustrates the emission spectrum of OH ($A^2\Sigma^+ \rightarrow X^2\Pi$, 0-0) under different applied voltage. The wavelength of four band heads for OH ($A^2\Sigma^+ \rightarrow X^2\Pi$) is 306.537 nm (R1), 306.776 nm (R_2), 307.844 nm (Q_1), 308.986 nm (Q_2) [12,13] respectively. From Fig. 2, it is obtained that the transition band around 309 nm is obvious. The emission intensity of OH around 309 nm increases with the applied voltage. The reason is that the increasing discharge voltage makes the collision ratio between high-energetic electron and H_2O increases. And it leads to generate more OH radical, which is helpful to improve the decomposition rate of naphthalene.

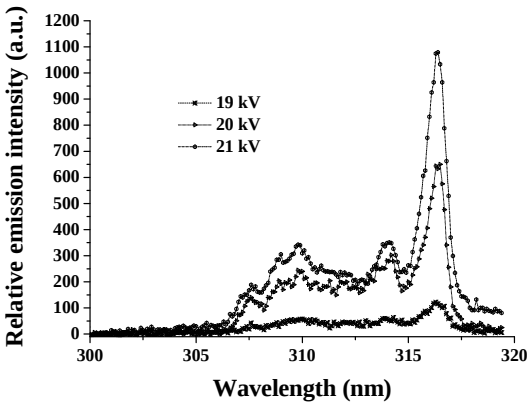

Fig. 2 Emission spectrum of OH under different applied voltage

3.2 The Effect of Humidity and Catalyst

There are many researches on the mechanism of plasma and catalyst combination at home and abroad [14-17]. In this work, in order to check the catalytic activity of catalysts, Mn coating (MnO_2) was selected as catalysts. It is coated on the negative board of the reactor.

Fig.3 illustrates the decomposing rate of naphthalene under catalyst of MnO_2 and the relative humidity of additional gas is 4% and 94% respectively. From Fig.3, it is indicated that the decomposing rate of naphthalene is higher under catalyst and high relative humidity. The reason can be explained as follow: Based on the Fenton-type reaction [18,19], H_2O_2 generates via the reaction between H_2O and O_2 in the discharge region and active radicals also generate via the reaction between Mn^{2+} or Mn^{4+} and H_2O_2. Therefore OH radical generates via Eq.(1)-(4) so as to improve the decomposing rate of naphthalene.

$$e^* + H_2O \rightarrow OH + H + e \quad (1)$$

$$2O_2 + 2H_2O \rightarrow O + OH + HO_2 + H_2O_2 \quad (2)$$

$$Mn^{2+} + 2H_2O_2 \rightarrow Mn^{4+} + 2OH + 2OH^- \quad (3)$$

$$Mn^{4+} + 2H_2O_2 \rightarrow Mn^{2+} + 2HO_2 + 2H^+ \quad (4)$$

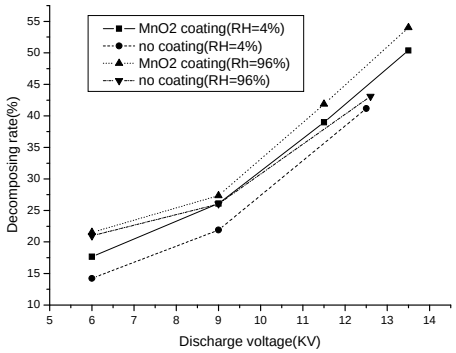

([Naphthalene] =30.5 mg/m^3)

Fig. 3 Naphthalene decomposition under different catalyst coat and humidity of additional gas

Eq.(1) is the main process of OH generation where e* represents the high-energetic electron. It is also obtained that the H_2O_2 is only generated via Eq.(2). And other active radicals will generate via the reaction between catalyst and H_2O_2. From the above analysis, it is concluded that the humidity of additional gas is a very important factor on generation of OH radical during the corona discharge. Therefore, the emission spectrum of OH radical was detected under different relative humidity. The result is illustrated in Fig.4. From the figure, it is obtained that the emission intensity of OH radical around 309nm increases obviously when the relative humidity increases. The reason is explained as follow: The main reaction of OH generation is Eq.(1). The collision rate between the high-energetic electron and H_2O increases with the increasing humidity. Hence, the collision velocity accelerates with the humidity and the OH radical concentration increases.

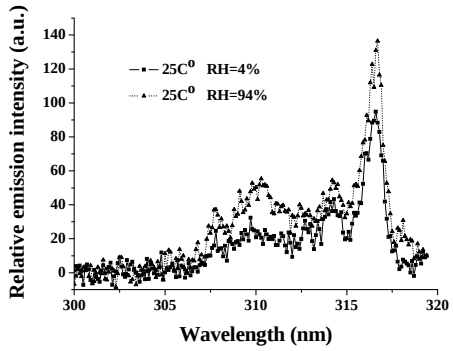

Fig. 4 Emission spectrum of OH under different humidity of additional gas

3.3 The Analysis Of By-products

The decomposition by-products of naphthalene were analyzed by the transform infrared spectroscopy (Necolet nexus spectrometer). The diagnostic peaks of naphthalene mainly distributes from 3124 cm^{-1} to 2890 cm^{-1}and from 917 cm^{-1} to 710cm^{-1}. FTIR analysis illustrated in Fig. 5 showed a decline of main naphthalene marker (absorption band around 3100 cm^{-1}) when the applied voltage increases from 0 kV to 14.5 kV. Therefore the decomposing rate of naphthalene improves with the applied voltage. On the other hand, FTIR spectral data in the CO_2 interference region (2400 cm^{-1}-2300 cm^{-1}) rises with the applied voltage. Therefore it is indicated that there is CO_2 generated.

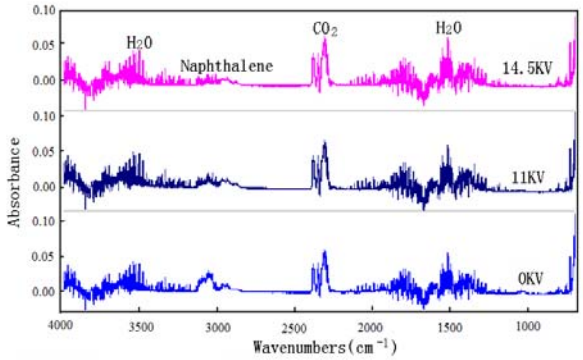

Fig. 5 FTIR diagram of naphthalene decomposition

In the decomposing process, there may be other by-products. However, the analysis is difficult since the concentration is very low and the absorption peak of H_2O will disturb the absorption peaks of other byproducts. Therefore, FTIR subtracting spectrum was used and the result is illustrated in Fig. 6. In Fig. 6, the positive peaks represent the by-products' generation (such as CO_2, CO, H_2O, etc) and the negative peak represents the decomposition of naphthalene. From the figure, it is obtained that the positive peak of CO_2 and H_2O is obvious. The result indicates that the main by-products in the decomposing process of naphthalene are H_2O and CO_2. From the FTIR subtracting spectrum there are a little of CO (absorption band: 2100cm^{-1}), ethylene (absorption band: 1940-1800cm^{-1}), methane (absorption band: 1400-1200 cm^{-1}), alcohol (absorption band: 3500-3200 cm^{-1}) and carboxylic acid (absorption band: 1760-1600cm^{-1}) to be found. In a word, the main by-product during the decomposition of naphthalene is CO_2 and H_2O. However, a little of CO and some small-molecule organic compounds can also be detected out because of the incomplete reactions.

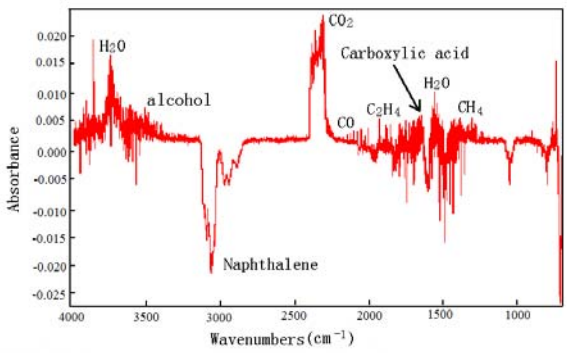

Fig. 6 FTIR subtracting spectrum of naphthalene decomposition

3.4 The Analysis of Decomposing Process of Naphthalene

The decomposing process of naphthalene with the corona discharge is very complicated. Fig. 7 indicates the bond length

of naphthalene. The bond length of naphthalene is different (I=0.136 nm, II=0.140 nm, III=0.139 nm, IV=0.142 nm) because of the different position of carbon atoms. The carbon atoms numbered 1, 4, 5 and 8 are called α position. The carbon atoms numbered 2, 3, 6 and 7 are called β position. The electron cloud density is high in α position; therefore the reactions always firstly occur in α position.

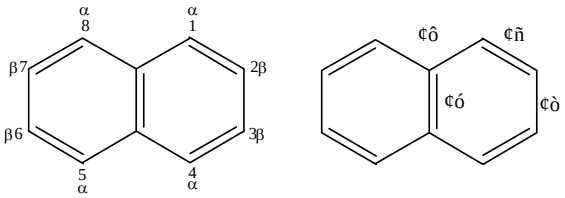

I=0.136 nm II=0.140 nm III=0.139 nm IV=0.142 nm

Fig. 7 The bond length of naphthalene

From the above investigation, the reaction between active radicals and naphthalene is a parallel and series-wound process [20]. The main decomposing processes are: (1) under the effects of active radicals such as OH, O, etc, the reactions firstly occur in α position. The C-H bond is broken. Naphthoquinone is formed via the pathway 2 via dehydrogenation and oxidation [21-23]. Then Naphthoquinone is oxidized into phthalic anhydride via the pathway 3 [23]. Subsequently, the maleic anhydride is formed as a significant product of phthalic anhydride via the pathway 4 [24]. Finally, a serial of radical reactions and oxidization reactions are gone and the pollutant is decomposed into CO_2, CO, H_2O, etc via the pathway 5; (2) the naphthalene is directly oxidized into phthalic anhydride via the pathway 1 [20] and then the pathways 4 and 5 happen. The naphthalene is finally decomposed into small molecules. Fig. 8 illustrates the concretely decomposing process of naphthalene. The main pathways of naphthalene decomposition are 1-4-7 and 2-3-4-7.

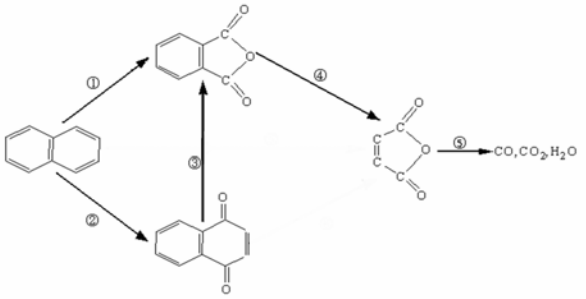

Fig. 8 Naphthalene decomposition process

The phthalic anhydride is an important intermediate product. The two pathways phthalic anhydride formed are pathway 1 and pathway 2-3 illustrated in Fig. 9 (a) and (b) respectively. In the processes, the dehydrogenation and oxidation mainly occur at α and β position to form phthalic anhydride. Then, the decomposition of phthalic anhydride is showed in Fig. 10. The maleic anhydride is formed via the broken of bonds [20]. Because the bond energy of C-O and C-C are low [25], the maleic anhydride can be decomposed into organic compounds such as carboxylic acid and alcohol. The carboxylic acid and alcohol have been detected in our experiments. Under the effects of active radical, these carboxylic acid and alcohol can be oxidized continuously into other small molecules such as alkane or olefin. Finally, CO_2 and H_2O were formed through further oxidation. In our experiment, CO_2 and H_2O can be found obviously.

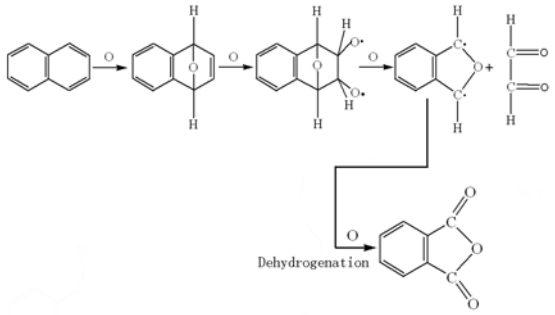

(a)

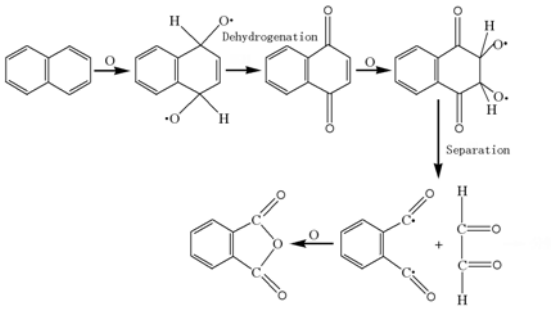

(b)

Fig. 9 Main reaction of phthalic anhydride formation

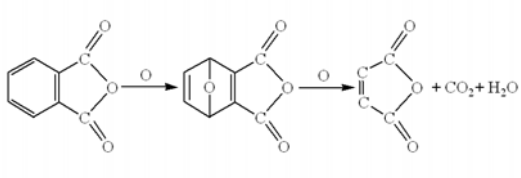

Fig. 10 Main reaction of maleic anhydride formation

4 CONCLUSIONS

The decomposition of naphthalene in the CRS system has been investigated. The high applied voltage and low initial concentration of naphthalene are helpful to decomposition. For the 17 mg/m^3 initial concentration of naphthalene, the decomposition rate reached 70% under 14kV applied voltage. The emission spectrum of OH ($A^2\Sigma^+ \rightarrow X^2\Pi$) as an important radicals has been detected out for naphthalene decomposition investigation. The increasing applied voltage and humidity can improve the amounts of OH generation. Moreover, the decomposing rate of electrodes coated by catalyst is higher than that of ordinary electrode. The analysis of by-products by FTIR and GC indicates that the main by-product is CO_2 and there are also little CO and other small-molecule compounds. The mechanism of naphthalene decomposition is a process of dehydrogenation and oxidation.

ACKNOWLEDGEMENTS

The work is supported by 973 Program of China (2006CB200303), 863 Project of china (2007AA061804), NSF of Zhejiang (Y507079), EOP of Zhejiang (Y200702725) and PSF of China (20080431325).

REFERENCES

1. D F. S. Natusch, Poly-cyclic Aromatic Hydrocarbons, 7th International Symposium on PAH, 951-959, 1983.
2. L. Roy and T. Bennett, Poly-cyclic Aromatic Hydrocarbons, 3rd International Symposium on PAH, 410-428, 1979.
3. J. M. Sontag, Carcinogens in Industry and Environment, Manel Dekker Inc., New York, 181-184, 1981
4. T. Hammer, B. Stefan, Plasma enhanced selective catalytic reduction of NO_x for diesel cars, SAE paper, No. 98848, 1998.
5. M. A. Jani, K. Takaki, T. Fujjwara, Rew. Sci. Insutru., 1998, 69(1): 1817-1849.
6. K. Urashima, J. S. Chang, IEEE Trans on Dielectrics and Electrical Indus., 2000, 7(5): 602-614.
7. Tata, S. Manni, Radiat. Phys Chem., 1993, 42(4-6): 701-710.
8. J Li, G F Li, Y Wu, N H Wang, Q N Huang, Journal of Environmental Sciences-Chinese, 2004, 16(1): 145-148.
9. Z L Wu, X Gao, Z Y Luo, E Z Wei, Y S Zhang, J Z Zhang, M J Ni and K F Cen, Energy & Fuels, 2005, 19: 2279-2286.
10. W C Wang, S Wang, F Liu, W Zhang, D Z Wang, Spectrochimica Acta Part A, 2006, 63: 477-482.
11. M Sun, Y Wu, J L Zhang, J Li, N H Wang, J Wu, Spectroscopy and Spectral Analysis 2005, 25(1): 108-112.
12. Charles de Izarra, Journal of Physics D: Applied Physics, 2000, 33: 1697-1704.
13. J. M. Cormier, S. Pellerin, F. Richard, K. Musiol, J. Chapelle, Journal of Physics D: Applied Physics, 1996, 29: 726-739.
14. T. Yamamoto, K. Mizuno, I. Tamori, A. Ogata, M. Nifuku, M. R. Prieto, IEEE Trans. on Ind. Appl., 1996, 32(1): 100-105.
15. Ogata, K. Yamanouchi, K. Mizuno, S. Kushiyama, T. Yamamoto, IEEE Trans. Ind. Appl. 1999, 35(6): 1289-1295.
16. Ogata, D. Ito, IEEE Trans. Ind. Appl., 2001, 37(4): 959-964.
17. Ogata, N. Shintani, IEEE Trans. Ind. Appl., 1999, 35(4): 753-759.
18. D. R. Grymonpre, W. C. Finney, R. J. Clark, B. R. Locke, Ind. Eng. Chem. Res., 2003, 42: 5117-5134.
19. Y. Flores, R. Flores, A. A. Gallegos, Journal of Molecular Catalysis A: Chemical, 2008, 281: 184-191.
20. J.K. Dixon, J.E. Longfield, Catalysis, VII, 1960, 183.
21. D. Vialaton, C. Richard, D. Baglio, Journal of Photochemistry and Photobiology A: Chemistry, 1999, 123: 15-19.
22. Lair, C. Ferronato, J. M. Chovelon, J. M. Herrmann, Journal of Photochemistry and Photobiology A: Chemistry, 2008, 193: 193-203.
23. J. A. Onwudili, P. T. Williams, Journal of Supercritical Fluids, 2007, 39: 399-408.
24. M. S. Wainwright, N. R. Foster, Catalysis Reviews, 1979, 19: 211-292.
25. Lopez, T. Bitzer, T. Heller, N. V. Richardson, Surface Science, 2001, 477: 219-226.